Phase-sensitive optical amplifier

D. R. Matthys
Marquette University, Milwaukee, Wisconsin 53233

E. T. Jaynes
Washington University, St. Louis, Missouri 63130
(Received 3 November 1977; revised 19 March 1979)

The application of Armstrong's super-regenerative principle to a laser amplifier shows that it is possible to control the phase of even a low-gain He-Ne laser amplifier by injecting as few as four or five photons just after the laser is turned on and while it goes through threshold. Estimation of the uncertainties in determining the level of the injected signal and the phase of the laser output indicates that measurements approaching the limit $\Delta n \Delta\phi \simeq 1/2$ may be possible.

INTRODUCTION

A high-gain linear (i.e., phase-sensitive) amplifier at optical frequencies would have many applications in communications and as a research tool. Previous efforts[1] to use a laser amplifier as a phase-measuring device have stressed the need for a high-gain laser such as a Nd:YAG system.

In the early days of radio, Armstrong's super-regenerative principle[2] made possible unlimited gain from a single vacuum tube stage of modest intrinsic gain. We have confirmed that the same principle, applied at optical frequencies, allows one to achieve any desired gain from the intrinsically low-gain helium–neon laser while retaining phase sensitivity. The following reports an experimental determination of the noise level of such an amplifier.

At low frequencies ($\hbar\omega \ll kT$) a theoretical limit on usable gain is set by thermal noise at the input as given by the Nyquist formula $P_N = kTB$ for the available noise power in a bandwidth B. Experimentally, super-regenerative amplifiers at both radio[3] and microwave[4] frequencies readily approach this limiting sensitivity.

At optical frequencies ($\hbar\omega \gg kT$) an often quoted theoretical limitation arising from quantum theory replaces the Nyquist formula by $P_Q = \hbar\omega B$. The physical origin of this "quantum noise" is ascribed variously[5–7] to spontaneous emission, zero-point field fluctuations, or the Heisenberg uncertainty principle. Also, Ross[7] has noted some qualitative differences in the nature of thermal noise and quantum noise.

For present purposes, we need not go into these matters beyond noting that, while the Nyquist thermal noise formula has been confirmed by innumerable experimental measurements, there appear to be no direct experimental tests of the quantum noise formula (of course, we have many measurements of related phenomena such as amplitude and phase fluctuations in cw lasers[8]). A measurement of the noise level of a super-regenerative optical amplifier is, therefore, of interest not only for determining its possible useful applications, but also because such a measurement might provide a direct test of some fundamental aspects of quantum theory, i.e., how does the attainable amplitude and phase measurability compare with the Heisenberg limit $\Delta n \Delta\phi \geq \frac{1}{2}$? (It should be pointed out here that this formulation of the Heisenberg principle for a fully quantized theory has been rejected,[9,10] but in a semiclassical treatment it follows easily from the usual $\Delta p \Delta q$ form.)

I. EXPERIMENTAL PROCEDURE

The physical setup used to obtain answers to these questions consisted of two He–Ne lasers operating in Gaussian mode at 633 nm arranged around a Mach–Zehnder interferometer as shown in Fig. 1. The cw laser was a Spectra-Physics Model 131 with dc excitation, while the pulsed laser amplifier was locally constructed and driven by a rf transmitter. Variations in frequency and amplitude due to thermal and other effects were negligible during the time required to record each sample. Due to different cavity dimensions, only one mode of each laser could interfere at any time with a mode of the other laser. The amplifier laser was turned on for about 100 μs at a 4-kHz repetition rate, by pulsing its 20-MHz rf excitation (cutting off the screen grid of the final amplifier stage). Part of the output from the cw laser was coupled into the cavity of the pulsed laser. If during the initial buildup of laser oscillation in the pulsed laser this injected signal is within the amplified frequency band and has a sufficient amplitude, then a definite phase relationship should exist between the original laser beam and the output of the pulsed laser. Oth-

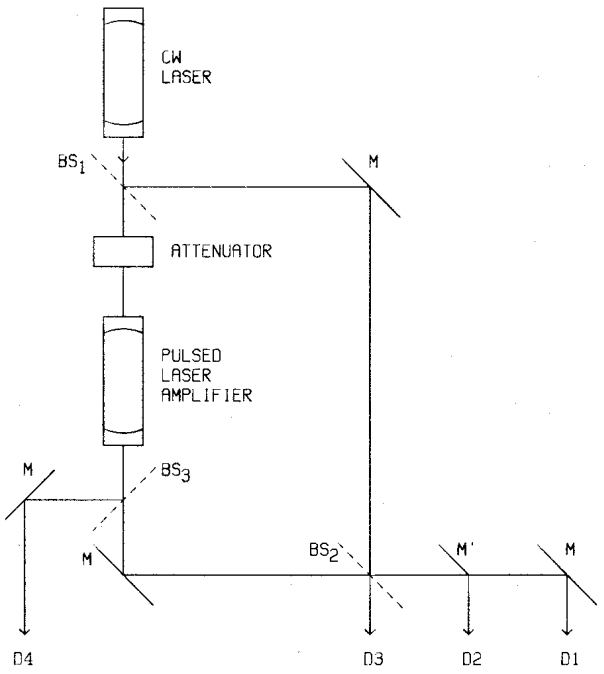

FIG. 1. Experimental arrangement of the two lasers and the interferometer. BS are beamsplitters; M are mirrors; M′ is special edge mirror cutting halfway into the beam; D1, D2, D3, D4 are photomultiplier tubes.

 0030-3941/80/030263-05$00.50

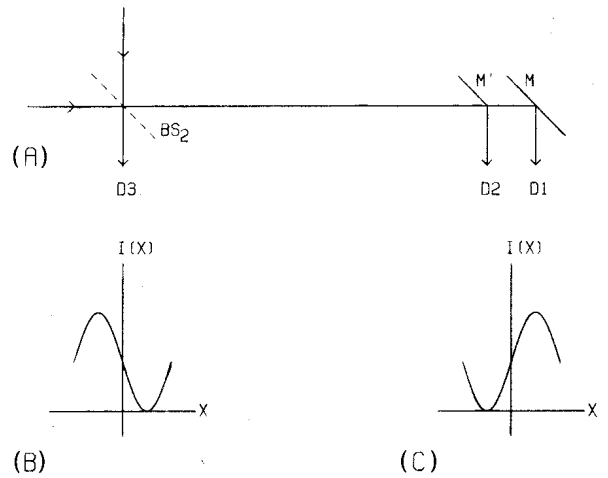

FIG. 2. (A) Detail of interferometer output showing detectors D1, D2, D3. (B) Plot of intensity variation across the output beam seen by D3. D3 then gives the total integrated intensity I_{D3}. (C) Plot of intensity variation across output as seen by D1 and D2. D1 sees only the right half of the beam and D2 sees only the left half. The integrated intensities of the two halves are I_{D1} and I_{D2}.

erwise, the phase difference between the two beams should vary randomly from pulse to pulse.

If it could be determined how much injected energy was present in the amplifier cavity at the time it was pulsed on, then monitoring the phase relationships in the interferograms produced at the two outputs of the interferometer would allow not only the determination of the minimum energy injection required for phase control, but also a measurement of the uncertainty product $\Delta n \Delta\phi$ for the injected signal.

To record the interferograms produced at each turn-on of the pulsed laser three EMI 9558B photomultipliers were used as detectors D1, D2, D3, arranged as shown in Fig. 2 to intercept the output signals. The glass–dielectric interface of the output beamsplitter BS_2 introduced a different phase shift for the reflected portion of the beam entering from the dielectric side than for the reflected portion of the beam entering from the glass side, so the two outputs are not the same but have a phase difference of 180° between them, i.e., they have the form $I = I_0\,(1 \pm \cos\phi)$, where ϕ is the phase difference at each point of the interferograms.

II. METHOD OF ANALYSIS

Since the output of each laser is restricted to the lowest-order Gaussian mode, the form of the electromagnetic field in the cw beam and in the output beam of the pulsed laser can be expressed in the forms

$$\overline{E}_1(r,t) = \overline{A}_1 \exp(-r^2/w_1^2)\cos\omega t, \tag{1}$$

$$\overline{E}_2(r,t) = \overline{A}_2 \exp(-r^2/w_2^2)\cos[\omega t + \phi(t)], \tag{2}$$

respectively. Here A_1, A_2 represent the maximum field strength at the center of the beams and w_1, w_2 are the beam radii at which the field strength has fallen to $1/e$ of the central maximum. It is assumed that the two frequencies are the same and that the phase difference $\phi(t)$ between the beams, though time-dependent, changes slowly with respect to the measurement time of the experiment. Adjusting the shear and tilt between the two beams will produce a linear variation of phase across the interference pattern at the outputs, such that the intensity over the plane transverse to the beams at the location of minimum shear is found to be

$$I(r) = \langle[\overline{E}_1(r,t) + \overline{E}_2(r,t)]^2\rangle_{\rm av}$$
$$= \tfrac{1}{2}\,[A_1^2\exp(-2r^2/w_1^2) + A_2^2\exp(-2r^2/w_2^2)]$$
$$+ A_1A_2\exp(-r^2/a^2)\cos\phi(r), \tag{3}$$

where

$$a^2 = w_1^2w_2^2/(w_1^2 + w_2^2) \tag{4}$$

is the effective beam size.

Adjusting the tilt between the beams changes the fringe spacing, of course, so if b is introduced as a parameter specifying the half-fringe spacing, ϕ_0 is the phase difference at the center of the pattern, and the fringes are specified as perpendicular to the x axis, then the total integrated intensity in the output beams is found to be

$$I = (\pi/4)(A_1^2w_1^2 + A_2^2w_2^2)$$
$$\pm 2A_1A_2a\sqrt{\pi}\int_0^\infty \exp(-x^2/a^2)\cos(\pi x/b)dx\cos\phi_0, \tag{5}$$

where the $\pm$ indicates the phase shift between the two outputs.

The first term is a constant background value and the second term contains all the interference effects. In this latter term, the first factor shows the effect of different beam sizes and power levels, and the exponential and cosine factors give the relationship between the half-fringe spacing b and the beam size w.

In order to obtain intensity and phase information in a form suitable for display on an oscilloscope, detectors D1, D2, and D3 are arranged as shown in Fig. 2. An edge mirror M′ is inserted into one of the output beams from the interferometer at BS_2, splitting the beam in half parallel to the fringes. Then the halves are sent to detectors D1 and D2. The other beam from the interferometer is sent to the detector D3. The total integrated intensity received at each of these detectors is

$$I_{D1} = (\pi/8)(A_1^2w_1^2 + A_2^2w_2^2)$$
$$-A_1A_2a\sqrt{\pi}\int_0^\infty \exp(-x^2/a^2)[\cos(\pi x/b)\cos\phi_0$$
$$+ \sin(\pi x/b)\sin\phi_0]dx, \tag{6}$$

$$I_{D2} = (\pi/8)(A_1^2w_1^2 + A_2^2w_2^2)$$
$$-A_1A_2a\sqrt{\pi}\int_0^\infty \exp(-x^2/a^2)[\cos(\pi x/b)\cos\phi_0$$
$$- \sin(\pi x/b)\sin\phi_0]dx, \tag{7}$$

$$I_{D3} = (\pi/4)(A_1^2w_1^2 + A_2^2w_2^2) - 2A_1A_1a\sqrt{\pi}$$
$$\times\int_0^\infty \exp(-x^2/a^2)\cos(\pi x/b)dx\cos\phi_0. \tag{8}$$

Subtracting the signals received at D1 and D2 gives

$$I_{D1} - I_{D2} = [-2A_1A_2a\sqrt{\pi}$$
$$\times\int_0^\infty \exp(-x^2/a^2)\sin(\pi x/b)\,dx]\sin\phi_0. \tag{9}$$

On the other hand, subtracting the signal at D3 from the combined signals from D1 and D2 leads to

$$I_{D1} + I_{D2} - I_{D3}$$

$$= [-4A_1A_2a\sqrt{\pi} \int_0^\infty \exp(-x^2/a^2)\cos(\pi x/b)\, dx] \times \cos\phi_0. \quad (10)$$

These equations for $I_{D1} - I_{D2}$ and $I_{D1} + I_{D2} - I_{D3}$ contain the desired information about intensity and phase difference in a form suitable for an X-Y display on a cathode ray oscilloscope. That is, by inserting proper gain factors, the signals (9) and (10) become proportional to $A_2 \sin\phi_0$ and $A_2 \cos\phi_0$, respectively, and the CRT display effectively draws the phase space diagram of the pulsed laser output, indicating simultaneously its amplitude and phase. The reproducibility of this on successive pulses then indicates how accurately the amplitude and phase of the injected signal are being determined by the pulsed amplifier.

The two equations involve integrals relating the effect of the beam-size to fringe-spacing ratio on the strength of the detected signal. Solving these integrals for equal balanced signals on the X-Y coordinates gives an optimum ratio of half-fringe spacing b to effective beam size a of $\pi a/2b = 1.1$. This value determines the proper adjustment of the interferometer for desired tilt between the beams.

However, it is also necessary to determine the level of the injected signal for each turn-on of the pulsed laser. This is obtained by monitoring the turn-on time of the laser amplifier. A slightly modified form of the equation of Sargent *et al.*[11] for the buildup of laser amplification is

$$d\langle n\rangle/dt = \alpha(\langle n\rangle + 1) - \beta\langle n\rangle - \kappa\langle n\rangle^2 \quad (11)$$

where α is the gain of the lasing medium, β represents the scattering and diffraction losses, κ is a phenomenological term added to account for saturation effects, and $\langle n\rangle$ is the photon number within the cavity. This equation predicts that a logarithmic plot of resonator energy versus time after turn-on would be logarithmic at very low levels, become linear over most of the interval from threshold to saturation, and then level off at saturation.

The effect of starting buildup from a low-level signal rather than from the noise level will be to shorten the time required to reach some specified level of laser output. If a reference level is chosen on the linear portion of the buildup curve well below saturation effects, and the gain of the laser is known, then a knowledge of how much the turn-on time was shortened allows a calculation of the injected energy present in the cavity when the laser began to turn on.

III. EXPERIMENTAL RESULTS

Figure 3 shows typical data obtained from pulsing the laser amplifier while an external signal was fed into it. The dotted line indicates the effect of removing the incoming signal.

The main body of the curve gives the distribution of turn-on times required to reach the reference level, while the left side of the curve indicates those pulses of the laser when lasing built up from energy coupled in from the external laser. The width of the main peak corresponds to fluctuations in the noise level of the laser amplifier and sets a limit of how closely

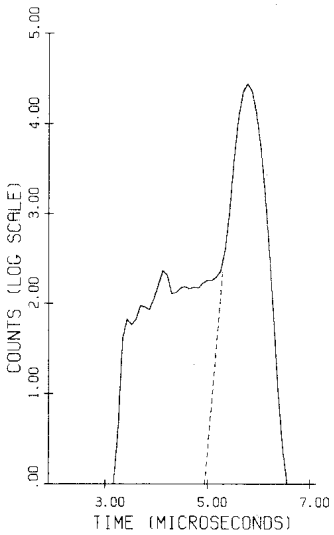

FIG. 3. Plot of time distribution curve for laser turn-on. Dotted curve shows results obtained when no signal is injected.

the shortening of turn-on time can be determined for any particular sample.

Referring back to Fig. 1, which gives the basic experimental layout, it is seen that part of the output from the laser amplifier is fed to a fourth detector D4. This last detector is coupled to a voltage comparator and a timing circuit so that information of the type shown in Fig. 3 can be collected.

Combining this information about turn-on times with the data obtained from the interferometer outputs allows a determination of the minimum signal required to control the laser amplifier and also an estimation of the uncertainty $\Delta n \Delta\phi$ in these measurements.

The attenuator used between the lasers as shown in Fig. 1 reduced the incident laser intensity by an order of magnitude, but much larger attenuation resulted from not matching the parameters of beam size and curvature for the two lasers. Since only minimal coupling was desired, the first laser was simply pointed down the cavity of the second laser. Aside from avoiding any direct reflections back into the pulsed laser cavity, no effort was made to prevent the possibility of scattered reflected light by the use of optical isolators. The pulsed laser, operating as a super-regenerative amplifier for any signal coupled into it at the time of turn-on, was pulsed at 4 kHz and the signals from the interferometer outputs and the timing signal marking time after turn-on of the laser amplifier were all recorded on tape. Since the available recorder was an incremental digital recorder, only about 50 samples per second, or about 1% of the signals, could be recorded.

It was found that there were three types of interferogram, shown in Fig. 4. These represented no interference and no coupling, interference but no coupling, and interference with coupling, respectively. The electronics at each detector was arranged so that 1.0 μA from each photomultiplier produced a 1.0-V signal. Under these conditions, the mean radius of the noise spot shown in the polar plot of Fig. 4 was 15 mV.

Because of thermal drift the two laser cavities were generally resonant at different frequencies. Thus by far the majority of the recorded data showed no interference, some showed interference without coupling (the two lasers interfered after the second laser had already turned on), and a few

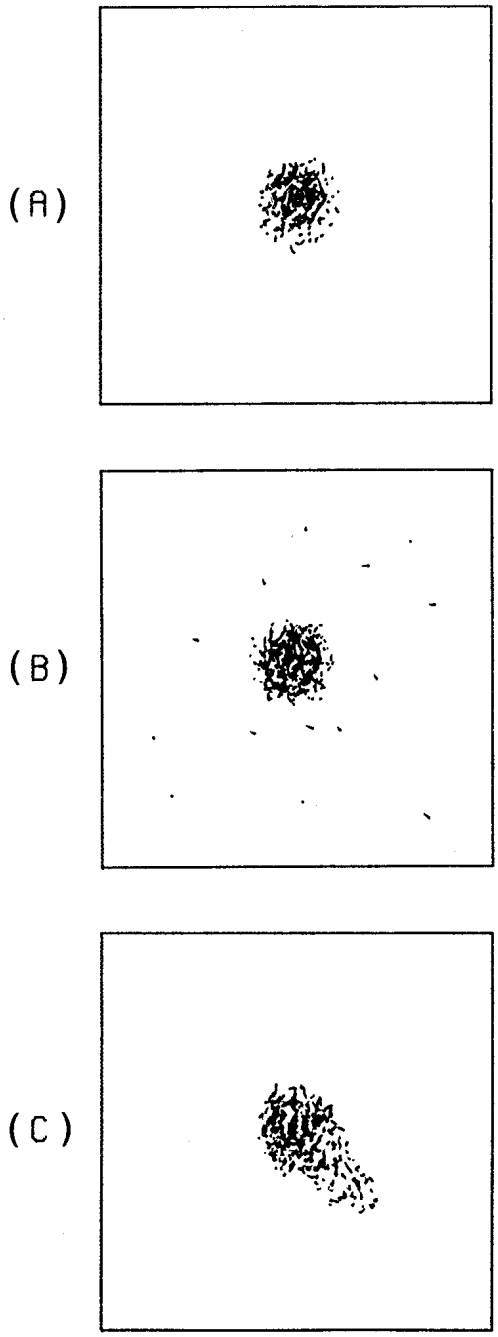

FIG. 4. Typical interference patterns. (A) No interference and no coupling. (B) Interference but no coupling. (C) Interference with coupling.

thousand samples showed both coupling and interference. Because of the large amount of background and the low recording rate, the results obtained do not have a large statistical reliability; however, using the shortened turn-on times as a criterion of coupling and utilizing only those samples that turned on well before the peak of the timing distribution curve, a small subset of several dozen samples still remained which allowed an estimate of the level of injected signal required to establish phase control of the second laser.

IV. DETERMINATION OF $\Delta\phi$ AND Δn

The uncertainty $\Delta\phi$ in measuring the relative phase between the interfering beams was caused by the statistical noise

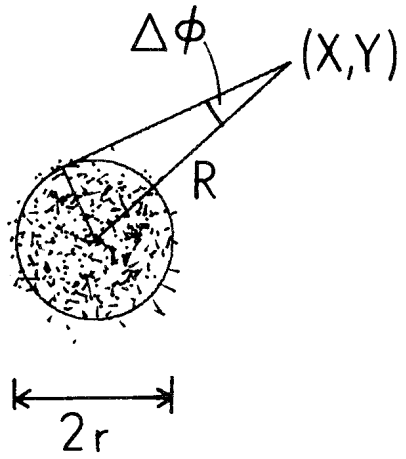

FIG. 5. Polar plot of intensity versus phase showing how the value of $\Delta\phi$ is determined by radius length R of sample at (X, Y) and the mean radius r of the central noise spot.

in the signals (cf. Fig. 5). Although the end point of the interference patterns for each signal could be readily determined, the exact origin of the signal was masked by the central noise spot. On the other hand, the uncertainty Δn in the determination of the injected signal is due to the finite width of the timing distribution curve for laser turnon. The problem is clearly seen by examining the solid-line curve of Fig. 3, which shows the timing distribution for laser turn-on with an injected signal. Lower levels of injected signal produce less shortening of the turn-on times and it becomes more difficult to assert that the early turn-on of a particular sample is due to the injected signal rather than to random fluctuations. In order to have reasonable confidence that the early turn-on is indeed due to the injected signal, only samples which turn on

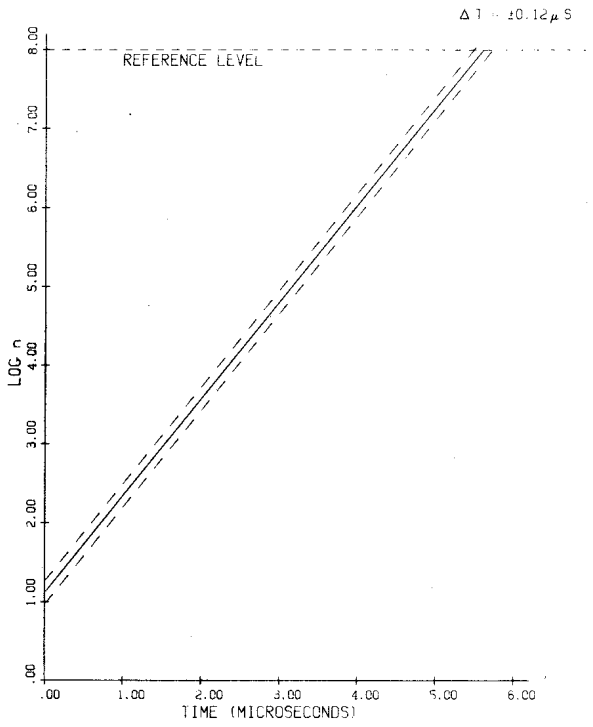

FIG 6. Plot of pulsed cavity energy versus time after turn-on for a particular sample that reached a reference level chosen well below saturation 5.6 μs after turn-on. n is energy in units of $\hbar\omega$.

at least four standard deviations ahead of the mean of the distribution curve are chosen. Staying this far out from the mean gives almost 100% probability that the sample is indeed responding to the injected signal.

In order to measure the energy level in the pulsed laser resonator when the laser is turned on, and also to estimate the uncertainty in this measurement, the timing information recorded by detector D4 for each sample is combined with the measured gain of the laser. As discussed earlier in reference to Eq. (11) the buildup of energy in the laser cavity is basically exponential until saturation effects become significant. If a reference level well below saturation is chosen, the cavity energy will build up to that level in exponential fashion. It is assumed that with no injected signal, the laser will build up from its noise level of about $\hbar\omega$ per mode,[12] so at $t = 0$, $n = 1$, where t is time after turn-on and n is the resonator energy expressed in units of $\hbar\omega$. This gives the peak at 6.6 μs in the timing distribution curve shown in Fig. 3. The fluctuations in noise give rise to the finite width of the peak, in this case a FWHM value of 0.12 μs.

An example is shown in Fig. 6 of a sample which reached the reference level in 5.6 μs, or 1 μs earlier than the peak. Extrapolating back from this point using the easily measured gain of the laser shows that this sample built up from a cavity energy of $n = 13$. Since the FWHM spread of the peak limits the accuracy with which the time shortening can be known, the sample turn-on time is bracketed by dashed lines 0.12 μs ahead and behind the measured turn-on time of 5.6 μs. Extrapolation from these values gives the uncertainty in the specification of the cavity energy at turn-on. For the sample shown, $n = 13$ with $\Delta n = +5, -4$. Using this procedure for all the samples that turned on sufficiently ahead of the timing distribution peak (four standard deviations was used as a criterion) shows that with an uncertainty in the injected signal of $\Delta n = 1.6$, as few as 4 or 5 photons were sufficient to control the laser amplifier. The corresponding uncertainty in measuring the phase difference for these same samples was about 0.3 rad. The range of $\Delta n \Delta\phi$ products obtained was from 0.4 to 0.7.

V. SUMMARY AND CONCLUSIONS

Even with the limited accuracy of these preliminary results, two conclusions are supported by this experiment. First, the extreme sensitivity of the super-regenerative amplifier system obviates the need for a high-gain laser in this type of phase-measuring setup. Only a few photons are required to establish phase control of the laser amplifier. Second, the uncertainty product $\Delta n \Delta\phi \approx 1/2$ which was obtained shows that the debate over various interpretations of Heisenberg's principle such as the Copenhagen interpretation,[13] the statistical interpretation,[14] and the challenge from those theories which reject field quantization[15] (which is usually regarded as the source of the resultant uncertainty) need not be regarded as purely theoretical or philosophical. Physical experiments within the bounds of present technology are capable of testing at least some of the many proposed interpretations.[16]

ACKNOWLEDGMENT

This work was supported in part by the AFOSR.

[1]H. Gerhardt, H. Welling, and D. Frölich, "Ideal laser amplifier as a phase measuring system of a microscopic radiation field," Appl. Phys. **2,** 91–93 (1973).
[2]E. Armstrong, "Some Recent Developments of Regenerative Circuits," Proc. IRE **10,** 244–260 (1922).
[3]F. E. Terman, *Radio Engineer's Handbook* (McGraw-Hill, New York, 1943), pp. 662–664.
[4]E. T. Jaynes, unpublished (1945). A 1-kW pulsed triode oscillator using a "lighthouse" tube at 1050 MHz was readily phase controlled by an injected cw signal at a level corresponding to energy $\approx kT$ in the tank circuit. This device proved to be the most sensitive microwave receiver available at the Naval Research Laboratory (Combined Research Group).
[5]A. Siegman, *Microwave Solid State Masers* (McGraw-Hill, New York, 1964), Chap. 8.
[6]R. Serber and C. H. Townes, "Limits on Electromagnetic Amplification Due to Complementarity," in *Quantum Electronics,* edited by C. H. Townes (Columbia University, New York, 1960), pp. 233–255.
[7]Monte Ross, *Laser Receivers* (Wiley, New York, 1966), pp. 29–32.
[8]K. Manes and A. Siegman, "Observation of quantum phase fluctuations in infrared gas lasers," Phys. Rev. A **4,** 373–386 (1971).
[9]L. Susskind and J. Glogower, "Quantum Mechanical Phase and Time Operator," Physics **1,** 49–61 (1964).
[10]P. Carruthers and M. Nieto, "Coherent states and the number-phase uncertainty relation," Phys. Rev. Lett. **14,** 387–389 (1965).
[11]M. Sargent, M. Scully, and W. Lamb, "Buildup of laser oscillations from quantum noise," Appl. Opt. **9,** 2423–2427 (1970).
[12]A. Siegman, *Introduction to Lasers and Masers* (McGraw-Hill, New York, 1971), p. 416.
[13]J. von Neumann, *Mathematical Foundations of Quantum Mechanics* (Princeton University, Princeton, N.J., 1955), Secs. IV.1–IV.2.
[14]L. Ballentine, "Statistical Interpretation of Quantum Mechanics," Rev. Mod. Phys. **42,** 358–381 (1970).
[15]E. Jaynes, "Survey of the Present Status of Neoclassical Radiation Theory," in *Coherence and Quantum Optics,* edited by L. Mandel and E. Wolf (Plenum, New York, 1973), pp. 35–81. See especially p. 36.
[16]D. Matthys, Ph.D. thesis, Washington University, St. Louis, Mo., 1975 (unpublished).